

Elsevier required licence: © <2021>. This manuscript version is made available under the CC-BY-NC-ND 4.0 license <http://creativecommons.org/licenses/by-nc-nd/4.0/>

The definitive publisher version is available online at

[\[https://www.sciencedirect.com/science/article/abs/pii/S1383586620320785?via%3Dihub\]](https://www.sciencedirect.com/science/article/abs/pii/S1383586620320785?via%3Dihub)

# Inkjet Printing of Graphene Oxide and Dopamine on Nanofiltration Membranes for Improved Anti-fouling Properties and Chlorine Resistance

Chen Wang<sup>1†</sup>, Myoung Jun Park<sup>1†</sup>, Dong Han Seo<sup>1</sup>, Ho Kyong Shon<sup>1\*</sup>

<sup>1</sup>School of Civil and Environmental Engineering, University of Technology, Sydney (UTS), City Campus, Broadway, NSW 2007, Australia

\* Corresponding author email: [Hokyong.Shon-1@uts.edu.au](mailto:Hokyong.Shon-1@uts.edu.au)

† Authors contributed equally to this work

## Abstract

Anti-fouling properties and chlorine resistance nature are highly desirable features for membranes used in nanofiltration (NF). Conventional polymeric NF membranes often suffer from fouling issues and poor stability under chlorine based chemicals. Therefore, in this work, a thin film composite (TFC) NF membrane was modified by coating a binding agent polydopamine (PDA) and graphene oxide (GO) using a simple and scalable inkjet printing process where the GO deposition was controlled by the number of printing cycles. The NF test results revealed the PDA-GO printed NF membranes exhibited higher salt rejection while achieving slightly lower permeate flux compared to control membrane. Moreover, the PDA-GO printed membrane exhibited enhanced anti-fouling properties where only 20% of permeate flux reduction was observed while the control membrane displayed significant reduction in flux up to 48%. Furthermore, chlorine resistance of the PDA-GO printed membrane showed reduction in salt rejection was effectively suppressed compared to the control membrane for the chlorination time of 1 and 3 hours. Our work demonstrates an effective strategy to mitigate fouling and chlorine stability issues in NF membranes as well as validate inkjet printing as a versatile technique for the formation of advanced nanomaterial based membranes with high controllability of membrane properties.

**Keywords:** Nanofiltration, Inkjet printing, Graphene oxide, Anti-fouling, Chlorine resistance

## 1. Introduction

Developing advanced TFC membranes for NF process has been an intensely researched topic over the last few decades due to their wide range of applications. Conventional TFC membranes are often fabricated by interfacial polymerization (IP) which forms a thin active layer on top of a microporous, thicker support substrates [1-3]. Properties of the active layer are is controlled by the IP process condition parameters including reaction time, temperature, monomer concentration, method to remove excess solution etc. Such conditions influence the pore size, porosity, thickness and morphology of the active layer, ultimately determining the membrane performances [4, 5].

For an ideal NF membrane, it needs to exhibit high permeate flux with high salt rejection capability. Moreover, it will be highly desirable if the membrane exhibits anti-fouling nature to fouling contaminants such as organics or biological species and display displays excellent stability against chlorine which is commonly used for membrane cleaning. Such chlorine agents can easily degrade the membrane lifetime and membrane performances. One alternative direction of research on developing desirable TFC NF membrane membranes with improved anti-fouling ability is surface modification of polyamide (PA) selective layer using nanomaterials. Especially, carbon nanomaterials having  $sp^2$  atomic structure such as graphene oxide (GO), carbon nanotubes, reduced graphene oxide, graphene quantum dots have been intensely studied, due to their advantages including its ability to provide low resistant pathway for water transport, excellent chemical stability and inertness, high abundance and anti-fouling properties properties [6-9]. Several modification methods including the surface grafting, cross-linking, dip coating and incorporation of nanomaterials to PA layer has have been adopted to enhance fouling propensity as well as chlorine resistance [10-13]. However, most of the surface modification processes often suffer from a controllability vs scalability dilemma where if the process provides a high controllability of the nanomaterial deposition, it often lacks the scalability or vice versa. More importantly, there are many chemicals and nanomaterials that are wasted during the modification process via conventional approaches [14]. Therefore, nanomaterial coating process which provides both scalability with high control of nanomaterial deposition with minimal production of wastes remains as a significant challenge in the advanced nanomaterial based membrane production.

Owing to such issues, recently, inkjet printing technique has been adopted as an effective and efficient way of depositing nanomaterials/polymer solutions with high control of nanomaterial

nanomaterials and membrane properties. Moreover, inkjet printing process is a widely adopted, scalable technology where its successful industry implementation was demonstrated in various fields, such as sensors, electronics, ceramics, biological cells and catalysts [15-19]. A few studies have been conducted to evaluate the feasibility of using inkjet printing technology in membrane field. Badalow et al. investigated the deposition of m-phenylene diamine (MPD) monomer using an inkjet printer onto an ultrafiltration (UF) support substrate before the IP process with trimesoyl chloride (TMC) monomer. Single and multiple coatings of MPD were successfully printed onto the UF support. Results showed that the permeate flux decreased while the salt rejection increased with increase in number of MPD printed layers [14]. Lee et al. utilized the inkjet printing technique to print silver nanoparticles on the surface of an electrospun polyurethane (PU) nanofiber. It was demonstrated that the nanofiber membrane was uniformly coated with silver nanoparticles and the modified membrane significantly inhibited the growth of different types of pathogens causing the water borne diseases [20]. Fathizadeh et al. studied the feasibility of using inkjet printing process to deposit GO flakes onto the modified polyacrylonitrile (PAN) support as an effective NF membrane. Compared with the commercial polymeric NF membranes, the GO modified membranes exhibited higher water permeability and higher rejection of small organic particles. Besides, the GO modified membranes also exhibited high rejection of pharmaceutical contaminants (95%) with small decline in water flux (10%) in the longevity test [21]. Li et al. investigated the inkjet printing to print DA and sodium periodate (SP) to deposit PDA onto a UF polypropylene (PP) membrane. Compared with the pristine PP membrane and only DA coated membrane, the PDA printed membrane exhibited higher water permeability and enhanced anti-fouling performance due to improvement of PDA oxidation degree [22].

In this study, we aimed to synthesize TFC-NF membrane membranes using an inkjet printing technology to coat GO nanoparticles on the surface of active layer to enhance the anti-fouling and chlorine resistance properties. Membrane fouling especially arising from the organic foulant is a significant issue in the NF application [23, 24]. Fouling in the membrane decreases permeate water quality, water recovery and shortens the lifespan of membranes. Currently, to handle the fouling problem, procedures such as regular pre-treatment of the feed solution and cleaning of the fouled membranes are implemented. However, these measures lead to increase in operation cost of the filtration processes and complicate the process [25-27]. Therefore, it is essential to develop the membranes with optimized surface properties with enhanced anti-fouling properties. Owing to such significant fouling issues, many strategies have been

implemented to reduce the fouling phenomena where novel anti-fouling materials are were introduced as parts of a membrane. One of such exemplary materials is GO which is a nanomaterial consists of sheets of  $sp^2$  carbons with presence of rich oxygen functional groups such as hydroxyl, carboxyl, ether and epoxy groups. Previous research has demonstrated that utilization of the GO flakes on the membrane surface could significantly reduce the fouling caused by the hydrophobic foulants [28]. Moreover, high chemical stability of the GO, significantly enhances the chemical stability of membrane which helps to protect the membrane from the degradation against the chlorine based agents and chemicals [29-31].

In this work, we developed an effective coating strategy using a simple and scalable inkjet printing technique to enable uniform coating of the GO leading to improve anti-fouling and chlorine resistant properties. Moreover, the printing of the DA on the membrane, which self-polymerised into PDA, acted as a strong binding agent between GO and PA active layer to make our composite membrane to be chemically and mechanically stable. The synthesized PDA-GO membranes were characterized and tested under the saline feed water to evaluate the membrane performances. Then the membrane fouling and chlorine stability tests were conducted and we observed that the membrane performances, anti-fouling properties and chlorine stability were enhanced by uniform coverage of the GO on the membrane surface with minimal GO usage. Furthermore, to the best of our knowledge, this research is the first demonstration of surface modification of NF membrane using GO and DA via inkjet printing printings. Our findings would enlighten further development of printing technology for surface modifications as well as for synthesizing advanced nanomaterial based NF membranes where high precision coating of nanomaterials is required.

## **2. Materials and methods**

### **2.1 Materials**

The commercial “NF90” NF membrane was purchased from Toray Chemicals, Republic of Korea. Graphene oxide (GO) powder was purchased from Graphenea. Dopamine hydrochloride, Tris(hydroxymethyl)aminomethane hydrochloride (Tris-HCl), sodium chloride (NaCl), bovine serum albumin (BSA) and sodium hypochlorite (NaOCl) were purchased from Sigma-Aldrich. All the chemicals were used as received. The de-ionized (DI) water was used in all experiments produced by a Millipore Milli-Q water system. A commercial Deskjet 2130 HP printer was used for printing the materials on the membrane surface.

## 2.2 Surface modification using inkjet printing

The NF90 membrane (membrane size: 6 cm × 6 cm) was taped to an A4-sized polyethylene terephthalate (PET) film and was loaded into the printer. A computer was connected to the printer and the printing software was set on paper type of glossy paper and maximum quality with 1200×1200 dpi. Firstly, the DA solution with a concentration of 0.21 mmol/mL was added into the cartridge and printed on the membrane surface. After the printing process, there was a transparent DA layer on the membrane surface. Then, the membrane was loaded into the printer again. The printing of GO solution with a concentration of 50 mg/L was performed. We printed the GO layer for 1, 2 and 3 times. The resultant PDA-GO membranes were referred to PDA-GO-1, PDA-GO-2 and PDA-GO-3, respectively. Finally, Tris-HCl buffer solution printing (50 mM, pH 8.8) took place as a last layer on the membrane surface to accelerate the self-polymerization of DA. The schematic illustration of the process is depicted in **Fig.1**. After final process, the membrane was dried at the controlled room temperature to ensure the cross linking between PDA and GO. During this time, the colour of membrane surface gradually became darker. In order to evaluate the stability of the PDA-GO membranes, we put a membrane sample in DI water for sonication (See **Fig.S1**). After the sonication, there was a negligible change of the membrane sample and we did not observe any GO particles released from the printed membrane demonstrating its good mechanical stability. For comparison, a membrane only printed DA and Tris-HCl solution was prepared and referred as a PDA-coated membrane. Detailed constitutions were presented in **Table 1**.

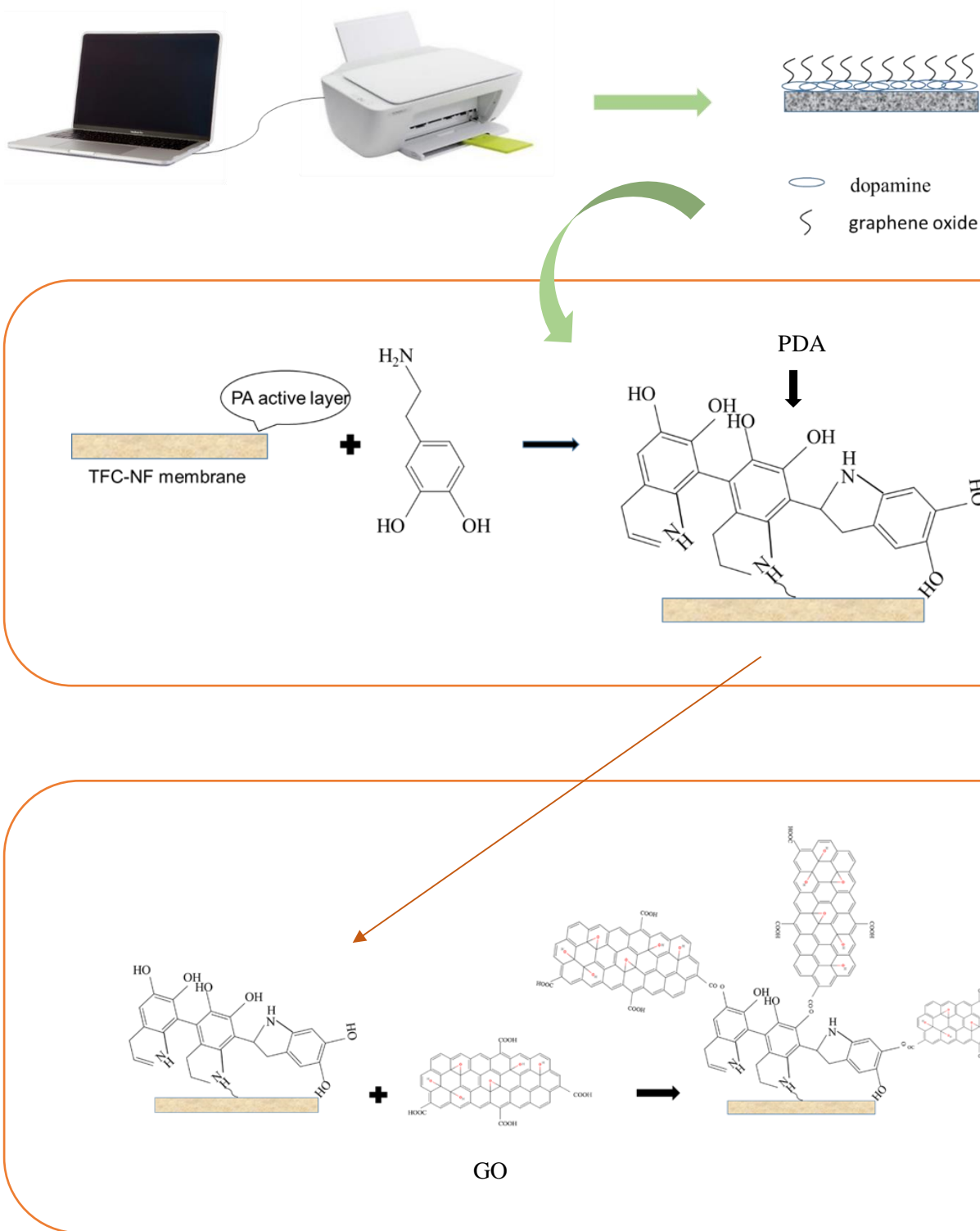


**Fig. 1** Schematic of the surface modification of NF90 membrane through inkjet printing technique.

**Table 1.** Specifications of the control and printed membranes

Membranes	DA (mmol/ml)	GO (50 mg/L)	Tris-HCl (mM)
Control	-	-	-
PDA-coated	0.21	-	50
PDA-GO-1	0.21	1 coating	50
PDA-GO-2	0.21	2 coatings	50
PDA-GO-3	0.21	3 coatings	50

### 2.3 Membrane characterization

Attenuated total reflection fourier transformed infrared spectroscopy (ATR-FTIR, Affinity-1 Shimadzu) was used to assess the functional groups of the membrane before and after the modification by inkjet printing. The membrane surface morphology and surface roughness were characterized by scanning electron microscopy (SEM, Zeiss Supra 55VP, Carl Zeiss AG) and atomic force microscopy (AFM, Park XE7), respectively. For the ATR-FTIR, SEM and AFM, each membrane sample was tested for three times in random positions of the membrane. The contact angle of the control and modified membranes were measured by the sessile drop method and analysed by the optical system (Theta Kite 100, Biolin Scientific) equipped with an image analysis software. For each membrane sample, the contact angle was recorded by the average data from three measurements in random positions on the membrane surface.

### 2.4 Membrane filtration tests

Membrane performance was evaluated with 1000 mg/L NaCl solution in a NF setup with an effective area ( $A$ ) of 4 cm<sup>2</sup>. Permeate flux and salt rejection were determined under the testing pressure of 6 bar at room temperature (23°C ± 1). At the beginning, the membrane was pre-compacted with DI water for 30 minutes [32]. After that, the permeate flux  $J_w$  was calculated by Eq. (1):

$$J_w = \frac{V}{A\Delta t} \quad (1)$$

where  $V$  is the volume of the permeate (L),  $A$  is the effective membrane area (m<sup>2</sup>), and  $\Delta t$  is the time interval (h).

Salt rejection  $R$  was calculated by Eq. (2):

$$R (\%) = 100 \times \left(1 - \frac{C_p}{C_f}\right) \quad (2)$$

where  $C_f$  and  $C_p$  are the salt concentrations in feed and permeate, respectively. Salt concentrations were measured by a conductivity meter.

## 2.5 Membrane fouling and cycling tests

Membrane fouling phenomena were investigated using a feed solution containing the BSA as model protein foulant. The BSA solution was prepared with a concentration of 200 mg/L and was constantly stirred on the magnetic stirrer for 24 hours before its use as a feed solution. Then the filtration tests were performed at the operating pressure of 6 bar under the room temperature. Firstly, the membrane was stabilized with DI water for 30 minutes. After the stabilization of the permeate flux, the feed solution containing BSA was introduced. Then the permeate flux was calculated at the time interval of 30 minutes. The relative permeate flux which is the measured permeate flux normalized by the initial flux was used to assess the degree of membrane fouling. For the membrane cycling tests, the BSA solution was again used as a feed solution with a concentration of 200 mg/L. Each fouling test was for each fouling test, the tests were performed for 120 minutes and the permeate flux was recorded at the time interval of 10 minutes. After each fouling test, the fouled membrane was cleaned for 30 minutes in the same NF setup using DI water as the feed solution.

## 2.6 Membrane chlorine stability tests

Chlorine stability tests were conducted by soaking the PDA-GO membranes and control membranes into the chlorine solution with different soaking time (1 and 3 hours). The chlorine solution was prepared by adding certain amounts of sodium hypochlorite into DI water to make the feed solution with a concentration of 6000 mg/L. After the chlorination, membranes were rinsed with DI water. Permeate flux and salt rejection of the control membrane and the PDA-GO membranes were measured with 1000 mg/L NaCl solution in a NF setup and compared to the membranes performance before the chlorination.

# 3. Results and discussion

## 3.1 Characterization of the printed PDA-GO-membranes

FTIR was performed to evaluate the functional groups of the control and printed membranes. As shown in **Fig. 2**, the pristine NF90 membrane exhibited characteristic peaks of typical PA active layer which is are located at  $1660\text{ cm}^{-1}$  (amide I, C=O stretching),  $1542\text{ cm}^{-1}$  (amide II, N-H in-plane bending), and  $1610\text{ cm}^{-1}$  (hydrogen bonded C=O) [33]. Compared to the control

NF90 membrane, the spectrum of the PDA-coated control membrane presented similar peak positions due to their similar chemical arrangement [34]. For the PDA-GO printed membranes, there was a pronounced peak located at  $1715\text{ cm}^{-1}$  (carboxylic acid C=O stretching) which mainly arose due to the presence of functional groups in GO such as carboxylic acid, hydroxyl, and amine groups [29]. Moreover, the peaks located at  $1610\text{ cm}^{-1}$  and  $3346\text{ cm}^{-1}$  (O-H functional group) disappeared due to the reaction between the carboxylic acid containing in GO interacting with amine and hydroxyl groups contained in PDA which is in good agreement with other literatures [35, 36].

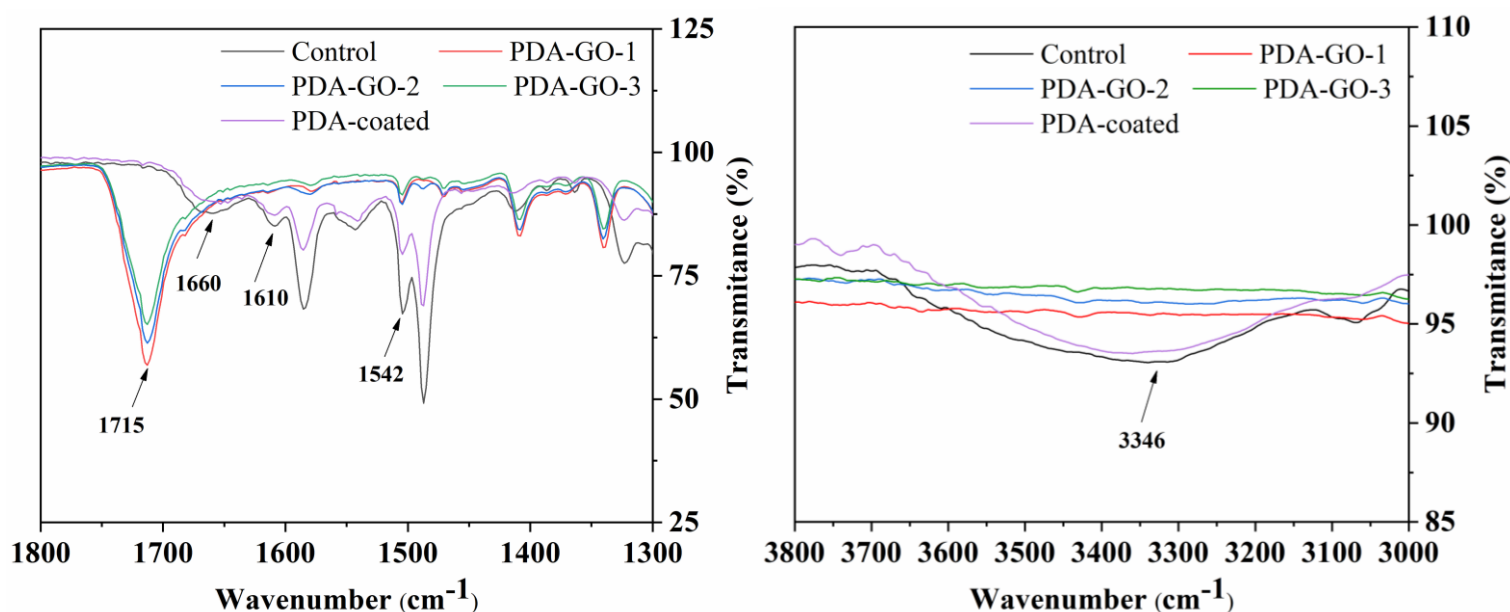


**Fig. 2** FT-IR spectra of the control and modified membranes.

Then the surface morphology analysis and the contact angle measurements were conducted and the results were compared between a control membrane sample and PDA-GO printed membranes (shown in **Fig. 3**). The surface of the control membrane showed a typical ridge-and-valley structure with highly porous, rough membrane surface. For the PDA-GO printed membranes, it is clear that as number of GO deposition increased, membrane surface became smoother and the number of visible valleys in the membranes were decreased. Such observation reveals that the printing of PDA-GO layers could potentially fill the valley regions of the NF membrane and making the membrane surfaces to become smoother.

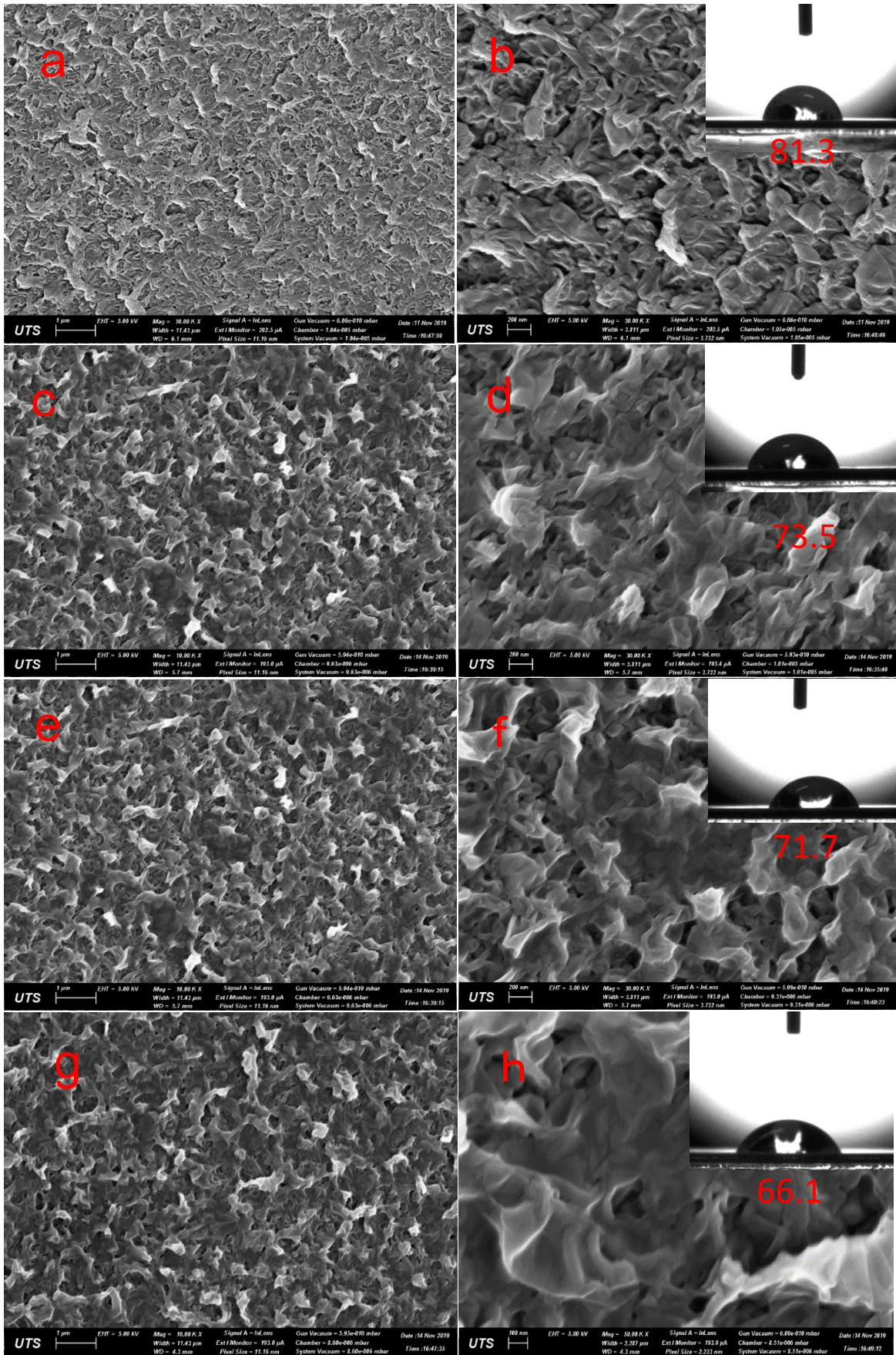


**Fig. 3** SEM images of membrane surfaces modified using inkjet printing of GO. (a) and (b) control NF90 membrane; (c) and (d) PDA-GO-1 membrane; (e) and (f) PDA-GO-2

membrane; (g) and (h) PDA-GO-3 membrane; Contact angle values were also included as an inset.

The contact angle measurement was carried out to evaluate the membrane affinity to water. The control membrane presented contact angle of  $81.3^\circ \pm 2^\circ$  whereas GO coating on the membrane led to lower contact angle of  $66.1^\circ \pm 1.7^\circ$  (PDA-GO-3 membrane) indicating that the PDA-GO membranes exhibit higher affinity with water. The improvement in the hydrophilicity arises mainly due to the oxygen-functional groups contained in the GO nanoparticles [37]. Moreover, we observed a consistent reduction in the contact angle values as number of GO printing layer was increased. Specifically, the contact angle value of PDA-GO-1 membrane was  $73.5^\circ \pm 2.4^\circ$  whereas contact angle value of PDA-GO-2 membrane was decreased to  $71.7^\circ \pm 2.6^\circ$  and further reduction to  $66.7^\circ \pm 1.7^\circ$  was observed for the PDA-GO-3 membrane. The list of contact angle data of the control and modified PDA-GO membranes can be found in **Table 2**.

**Table 2.** Contact angle of the control and printed membranes.

Membranes	Contact angle ( $^\circ$ )
Control	$81.3 \pm 2.0$
PDA-coated	$61.0 \pm 1.6$
PDA-GO-1	$73.5 \pm 2.4$
PDA-GO-2	$71.7 \pm 2.6$
PDA-GO-3	$66.1 \pm 1.7$

In order to characterize the membrane surface topography, AFM was conducted on the control and modified PDA-GO membranes (see **Fig. 4**). The AFM analysis revealed that the PDA-GO membranes had a smoother surface (surface roughness ranging from 23.3 nm to 36.2 nm) compared to the control NF membrane (surface roughness value of 44.2 nm). Such reduction in surface roughness arises due to GO particles filling the valley regions of the membrane surface and it is well supported by other characterization results [6, 38]. Moreover, the average surface roughness (Ra) value of the PDA-GO-printed membrane decreased with increase in number of GO printing layers. Specifically, the Ra value of the PDA-GO-1, PDA-GO-2 and PDA-GO-3 membranes were 33.6, 30.9 and 23.3 nm, respectively.

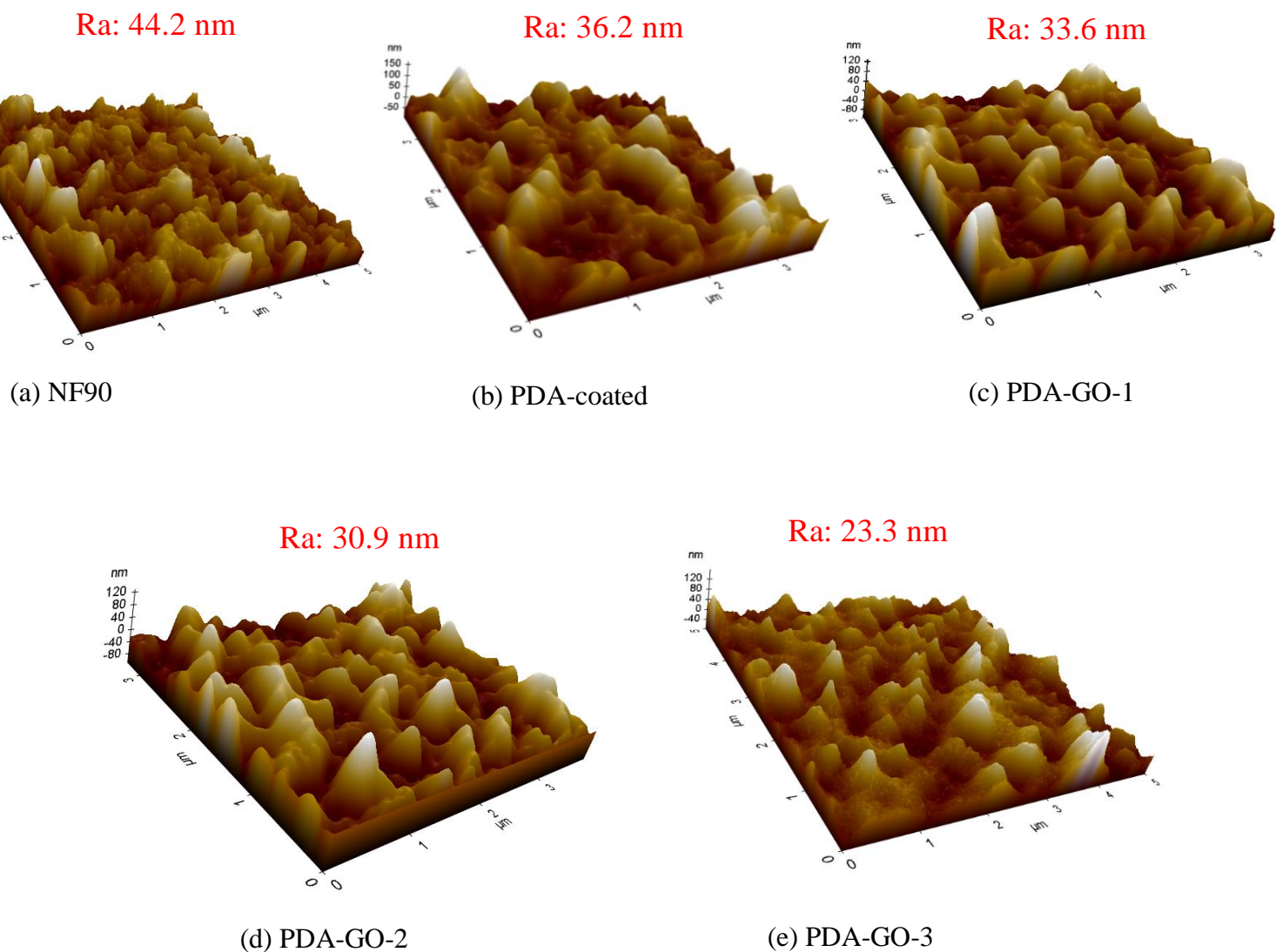


**Fig. 4** AFM images of membranes. (a) Control NF90 membrane; (b) PDA-coated membrane; (c) PDA-GO-1 membrane; (d) PDA-GO-2 membrane; (e) PDA-GO-3 membrane.

### 3.2 Membranes performance

To investigate the effect of GO printing on the NF membrane performance, water desalination tests were conducted using the saline feed water while measuring the permeate flux and salt rejection of the control and the PDA-GO-printed membranes. As shown in **Fig. 5**, compared to the control NF90 membrane, the permeate fluxes of the PDA-GO-printed membranes were slightly decreased while the salt rejection rates were increased. The permeate flux and salt

rejection of the control membrane was 13.32 LMH/bar and 90.72%, respectively. However, when PDA (PDA-coated) was coated on the PA layer, the flux slightly decreased to 11.49 LMH/bar while the salt rejection increased to 92.33% compared to the control membrane. These results may arise due to the increase in hydrodynamic resistance when PDA layer is formed via self-polymerization of DA which could play an essential role as an additional separation barrier. Thus, such PDA coating might slightly reduce pore size of the PA selective layer leading to a reduction in water flux while increasing salt rejection [39]. For the PDA-GO-printed membranes, it exhibited comparable changes in permeate flux value of 11.63 LMH/bar and salt rejection of 92.42% for PDA-GO-1 membrane, PDA-GO-2 membrane exhibited the flux of 11.22 LMH/bar and salt rejection of 92.65%, and PDA-GO-3 membrane showed that of 10.28 LMH/bar and salt rejection of 93.05%, respectively, compared to a PDA-coated membrane. These results are in good agreements with the previous researches that controlled amount of GO coating did not deteriorated the separation performance compared to a control membrane [28, 29, 40].

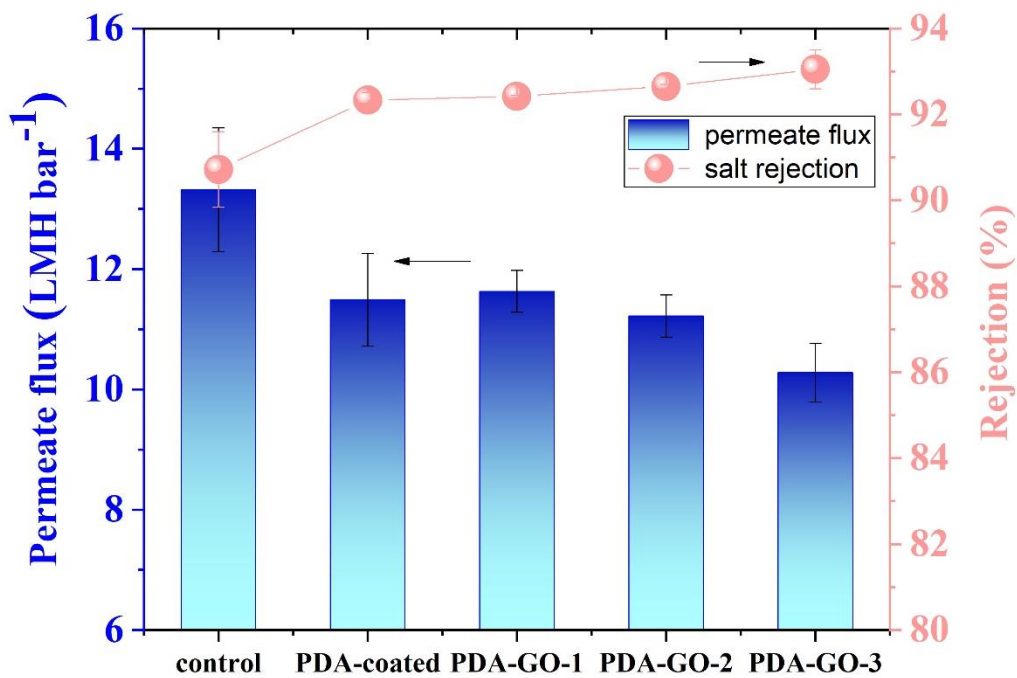


**Fig. 5** Permeate flux and salt rejection performance of a series of membranes. Test conditions: 1000 ppm NaCl as feed solution, pressure 6 bar, room temperature.

### 3.3 Membrane fouling and cycling tests

Membrane fouling is one of the major challenges for the membrane separation processes, which will affect the membrane **performances performance**. The reasons behind the membrane fouling are complex and many factors affect the fouling phenomena including the types of the foulants, experimental conditions and the membrane properties etc. For a NF membrane, hydrophilic and smooth surface is expected to enhance the anti-fouling property [25, 41]. Therefore, previous researches focused on enhancing the hydrophilicity of membranes by surface modification, membrane material modification and introducing different polymer blends. Among these approaches, applying the hydrophilic material or nanoparticles has been recognised as an effective and convenient way to enhance the membrane anti-fouling properties [42-44].

In our study, we have chosen coating of DA and GO nanoparticles on the PA selective layer of NF membrane to enhance the anti-fouling properties. In order to demonstrate the enhanced anti-fouling properties, the relative permeate flux over time of the control, only PDA-printed and PDA-GO-printed membranes were recorded using **a** 200 mg/L BSA as a feed solution (shown in **Fig. 6**). For the control membrane, the permeate flux decreased rapidly. At the end of the filtration time of 3 hours, the permeate flux became relatively stable. On the other hand, the permeate flux of the PDA-GO printed membranes exhibited slower reduction in the permeate flux. Moreover, the PDA-GO printed membranes showed a lower degree of final permeate flux reduction (20% to 30%) at the end of the filtration process compared to the control membrane (~48%) proving the enhanced anti-fouling properties. The improved anti-fouling properties could be attributed to the reduced surface roughness and enhanced surface hydrophilicity induced by the printing of DA and GO on the membrane surface. Hydrophilic surface could adsorb water molecules and then form a water layer on the surface, which could mitigate the adsorption of foulants and increase the fouling resistance to BSA [45]. Furthermore, smoother membrane surface minimizes the possibility of BSA molecules being firmly binding on the membrane surface [46, 47]. Amongst the PDA-GO-printed membranes, the anti-fouling properties were enhanced with increase in the number of GO printing layers. For example, the final permeate flux reduction for PDA-GO-1, PDA-GO-2 and PDA-GO-3 membranes was 28%, 24% and 20%, respectively. The increased anti-fouling properties may arise due to the enhanced hydrophilicity and the smoother surface formation as GO layers are increased (see **Fig. 3** and **Fig. 4**). PDA-printed membrane exhibited the final permeate flux

reduction of 32%, which demonstrates that addition of GO layers was critical in improving the anti-fouling properties of the membrane. From our experimental results and analyses we can deduce that the hydrophilicity is not the sole factor determining the membrane fouling but the combination of surface properties and membrane properties plays an important role in determining the fouling degree and its effects.

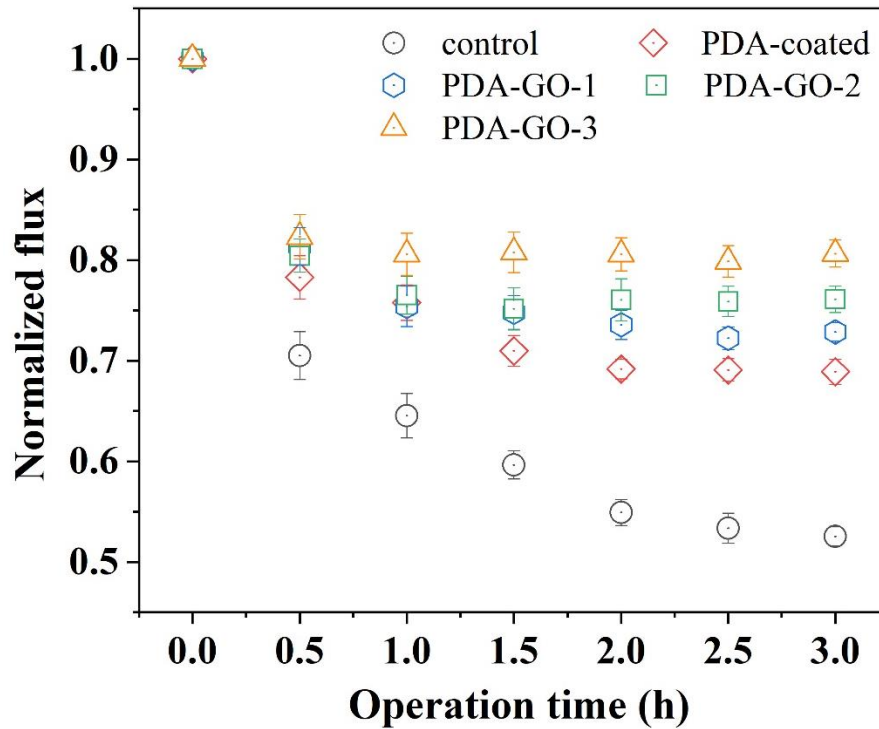


**Fig. 6** Normalized permeate flux of the control and modified membranes as a function of operation time upon the addition of 200 mg/L BSA at 6 bar.

In order to investigate the fouling reversibility and stability of the PDA-GO printed membranes under the fouling condition, we performed three cycles of fouling experiments where cleaning of the membrane was performed after each test. Then the normalized permeate flux was measured for each test and was compared between the PDA-GO membrane and the control membrane. The PDA-GO-3 membrane was chosen as the representative PDA-GO-printed membrane based on its excellent anti-fouling performance compared to other PDA-GO printed membranes. As shown in **Fig. 7**, the permeate flux of both control and PDA-GO-3 membranes cannot be fully recovered to their initial conditions even after the rigorous physical cleaning with DI water. This may be due to the adsorption of BSA foulants on the membrane surface, which is difficult to be completely removed by simple hydraulic cleaning [48]. The permeate

flux recovery values for control membrane were 62.8% and 57.6% in these three cycles whereas the significantly enhanced flux recovery was observed for the PDA-GO-3 membrane, where the normalized permeate flux of the 2<sup>nd</sup> and 3<sup>rd</sup> cycle tests exhibited values of 85.3% and 80.1%, respectively. These findings demonstrate that the PDA-GO-3 membrane would indicate good anti-fouling properties along with enhanced flux recovery (good reversibility), exhibiting stable performance under long-term operation compared to the pristine polymeric based control membrane.

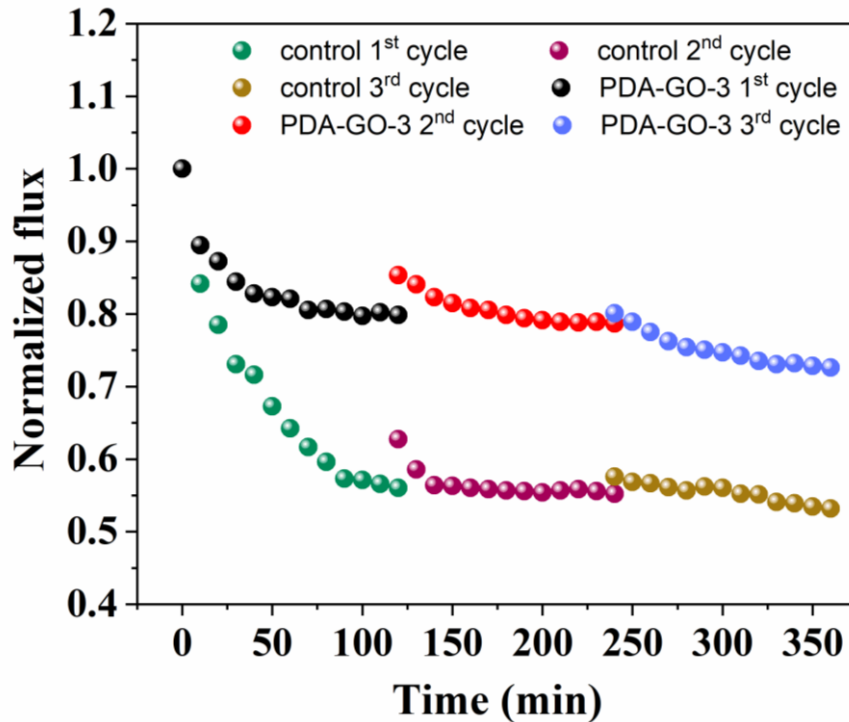


**Fig. 7** Recycling properties of control NF90 and PDA-GO-3 membranes. Test conditions: 200 mg/L BSA as feed solution, pressure 6 bar, room temperature.

### 3.4 Chlorine stability tests

After the fouling experiments, chemical stability of PDA-GO-printed membranes in the presence of chlorine was further evaluated. The control and PDA-GO-3 membranes were immersed in a high concentration solution containing 6000 mg/L NaOCl at pH 11 for 1 and 3 hours, the permeate flux and salt rejection after a certain duration of chlorination were measured with 1000 mg/L NaCl solution (shown in **Fig. 8**). Compared to the control membrane, effect of the chlorine chemical was less severe for the case of PDA-GO-3 membrane where reduction in salt rejection was less pronounced for the PDA-GO-3 membrane case. For the

chlorination exposure of 1 and 3 hours, the addition of GO layers in the modified membrane induced a negligible change in salt rejection membrane performance while control membrane exhibited degradation in salt rejection the membrane performances. In particular, the salt rejection of PDA-GO-3 membrane remained almost unchanged of 92.39% and 92.08% for 1 and 3 hours, respectively, compared to the membrane before chlorination (93.05%). For the control membrane, salt rejection decreased to 88.88% and 87.66% for 1 and 3 hours, respectively, compared to the value before chlorination (90.72%). Such observation arises due to the chemically inert nature of GO, acting as a protective layer for the inner polymeric part of the membrane from the active chlorine species ( $\text{OCl}^-$ ) penetration [28, 49]. Under the chlorination condition, for the control NF 90 membrane, the amide N-H group on the PA layer is transformed into N-Cl group, due to the lack of protons, the inter-chain hydrogen bonds is difficult to form. The absence of hydrogen bond leads to the enhancement of the chain mobility and the conformational alternation of polyamide structure, leading to rapid transport of salt ions and the salt rejection decreases [50-52].

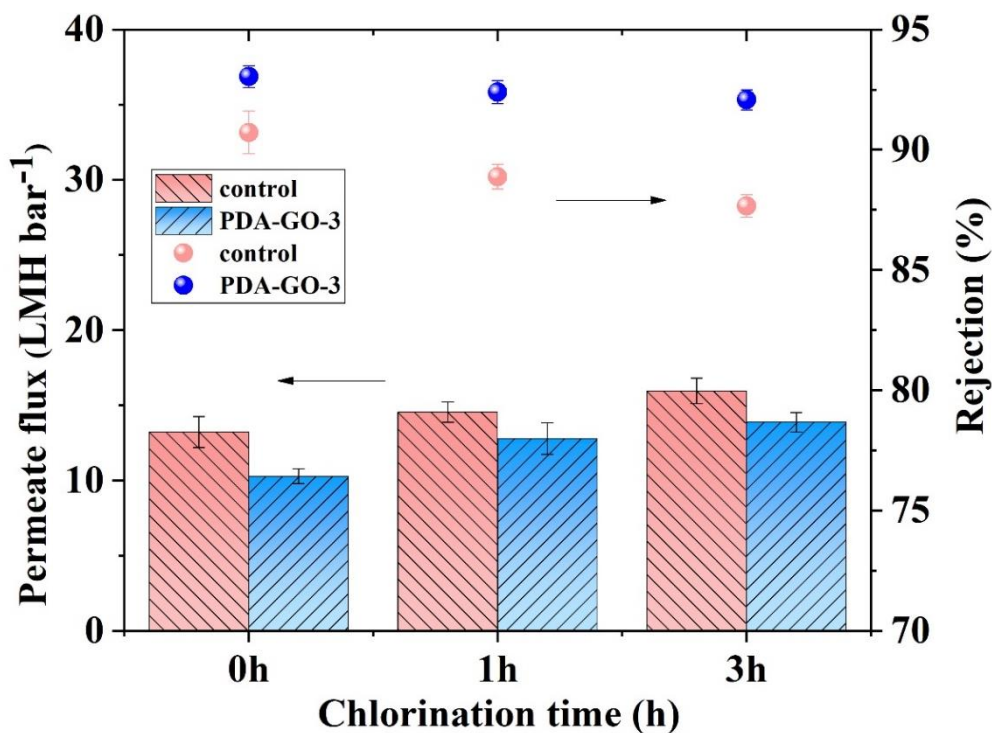


**Fig. 8** Permeate flux and salt rejection of control and PDA-GO-3 membranes as a function of the chlorination time. (Chlorination condition: 6000 ppm NaOCl).

Compared to the previous studies, the chlorination condition used in our tests (NaOCl 6000 ppm) was harsher. Previous researches used the concentration of NaOCl ranging from 10 to

100 ppm [50, 53]. Despite of chlorination in such harsh condition, the PDA-GO-3 membrane maintained the salt rejection around 92% up to the chlorination time of 3 hours, demonstrating good membrane performance and enhanced chemical stability of the PDA-GO-3 membrane, where the PDA-GO-3 membrane is also expected to display stable membrane performance if the chlorination condition is milder as used in previous studies.

#### **4. Conclusions**

In summary, we developed a PDA and GO composite NF membrane using a simple and versatile inkjet printing technique. Developed PDA-GO printed membranes exhibited slightly lower permeate flux while showing a higher salt rejection performance compared to the control polymeric NF membrane. For the membrane fouling tests, the PDA-GO printed membranes demonstrated improved antifouling properties compared to the control NF membrane. Similarly, for the chlorine stability tests, overall membrane performance was better maintained compared to the control NF membrane, due to chemically inert nature of the GO which retards the degradation of membrane induced by chlorine species. Overall, our work demonstrates that printing technology could serve as a simple and scalable way to effectively deposit functionalized nanomaterials and chemicals on the membrane surface with high precision. Moreover, our research findings shed a light on unique advantages of 2D nanomaterials in NF application and pave a way for the next generation 2D material based membranes for pressure driven water purification systems.

#### **Acknowledgements**

The authors thank Prof. Yuan Chen for material and assistance during this work. We thank the support of this research by the Australian Research Council (ARC) Industrial Transformation Research Hub (IH170100009). D.H.S acknowledges the support of Chancellor's postdoctoral research fellow scheme from UTS.

#### **References**

[1] Z. Zhang, G. Kang, H. Yu, Y. Jin, Y.J.D. Cao, From reverse osmosis to nanofiltration: precise control of the pore size and charge of polyamide membranes via interfacial polymerization, *Desalination*, 466 (2019) 16-23.

- [2] Q. Li, Z. Liao, X. Fang, J. Xie, L. Ni, D. Wang, J. Qi, X. Sun, L. Wang, J.J.D. Li, Tannic acid assisted interfacial polymerization based loose thin-film composite NF membrane for dye/salt separation, *Desalination*, 479 (2020) 114343.
- [3] T. Ormanci-Acar, F. Celebi, B. Keskin, O. Mutlu-Salmanlı, M. Agtas, T. Turken, A. Tufani, D.Y. Imer, G.O. Ince, T.U.J.D. Demir, Fabrication and characterization of temperature and pH resistant thin film nanocomposite membranes embedded with halloysite nanotubes for dye rejection, *Desalination*, 429 (2018) 20-32.
- [4] K.P. Lee, G. Bargeman, R. de Rooij, A.J. Kemperman, N.E.J.J.o.m.s. Benes, Interfacial polymerization of cyanuric chloride and monomeric amines: pH resistant thin film composite polyamine nanofiltration membranes, *Journal of Membrane Science*, 523 (2017) 487-496.
- [5] Z. Yao, H. Guo, Z. Yang, C. Lin, B. Zhu, Y. Dong, C.Y.J.D. Tang, Reactable substrate participating interfacial polymerization for thin film composite membranes with enhanced salt rejection performance, *Desalination*, 436 (2018) 1-7.
- [6] X. Huang, K.L. Marsh, B.T. McVerry, E.M. Hoek, R.B. Kaner, Low-Fouling Antibacterial Reverse Osmosis Membranes via Surface Grafting of Graphene Oxide, *ACS Appl Mater Interfaces*, 8 (2016) 14334-14338.
- [7] W. Yang, H. Xu, W. Chen, Z. Shen, M. Ding, T. Lin, H. Tao, Q. Kong, G. Yang, Z.J.D. Xie, A polyamide membrane with tubular crumples incorporating carboxylated single-walled carbon nanotubes for high water flux, *Desalination*, 479 (2020) 114330.
- [8] D.L. Zhao, T.S. Chung, Applications of carbon quantum dots (CQDs) in membrane technologies: A review, *Water Res*, 147 (2018) 43-49.
- [9] Y. Zhao, K. Tang, H. Ruan, L. Xue, B. Van der Bruggen, C. Gao, J.J.J.o.m.s. Shen, Sulfonated reduced graphene oxide modification layers to improve monovalent anions selectivity and controllable resistance of anion exchange membrane, *Journal of Membrane Science*, 536 (2017) 167-175.
- [10] M.L. Marré Tirado, M. Bass, M. Piatkovsky, M. Ulbricht, M. Herzberg, V. Freger, Assessing biofouling resistance of a polyamide reverse osmosis membrane surface-modified with a zwitterionic polymer, *Journal of Membrane Science*, 520 (2016) 490-498.
- [11] H.H. Rana, N.K. Saha, S.K. Jewrajka, A.J.D. Reddy, Low fouling and improved chlorine resistant thin film composite reverse osmosis membranes by cerium (IV)/polyvinyl alcohol mediated surface modification, *Desalination*, 357 (2015) 93-103.

- [12] Y.-N. Kwon, S. Hong, H. Choi, T.J.J.o.m.s. Tak, Surface modification of a polyamide reverse osmosis membrane for chlorine resistance improvement, *Journal of Membrane Science*, 415 (2012) 192-198.
- [13] X. You, T. Ma, Y. Su, H. Wu, M. Wu, H. Cai, G. Sun, Z.J.J.o.M.S. Jiang, Enhancing the permeation flux and antifouling performance of polyamide nanofiltration membrane by incorporation of PEG-POSS nanoparticles, *Journal of Membrane Science*, 540 (2017) 454-463.
- [14] S. Badalov, C.J. Arnusch, Ink-jet printing assisted fabrication of thin film composite membranes, *Journal of Membrane Science*, 515 (2016) 79-85.
- [15] W.L. Zhang, H.J. Choi, H.-S. Ko, K.-S.J.J.o.I. Kwon, E. Chemistry, Ink-jetting and rheological behavior of a silica particle suspension, *Journal of Industrial and Engineering Chemistry*, 22 (2015) 120-126.
- [16] W. Shen, X. Zhang, Q. Huang, Q. Xu, W.J.N. Song, Preparation of solid silver nanoparticles for inkjet printed flexible electronics with high conductivity, *Nanoscale*, 6 (2014) 1622-1628.
- [17] F. Torrisi, T. Hasan, W. Wu, Z. Sun, A. Lombardo, T.S. Kulmala, G.-W. Hsieh, S. Jung, F. Bonaccorso, P.J.J.A.n. Paul, Inkjet-printed graphene electronics, *ACS Nano*, 6 (2012) 2992-3006.
- [18] H. Minemawari, T. Yamada, H. Matsui, J.y. Tsutsumi, S. Haas, R. Chiba, R. Kumai, T.J.N. Hasegawa, Inkjet printing of single-crystal films, *Nature*, 475 (2011) 364.
- [19] S. Wang, N. Liu, J. Tao, C. Yang, W. Liu, Y. Shi, Y. Wang, J. Su, L. Li, Y.J.J.o.M.C.A. Gao, Inkjet printing of conductive patterns and supercapacitors using a multi-walled carbon nanotube/Ag nanoparticle based ink, *Journal of Materials Chemistry A*, 3 (2015) 2407-2413.
- [20] S.J. Lee, D.N. Heo, M. Heo, M.H. Noh, D. Lee, S.A. Park, J.-H. Moon, I.K. Kwon, Most simple preparation of an inkjet printing of silver nanoparticles on fibrous membrane for water purification: Technological and commercial application, *Journal of Industrial and Engineering Chemistry*, 46 (2017) 273-278.
- [21] M. Fathizadeh, H.N. Tien, K. Khivantsev, J.-T. Chen, M. Yu, Printing ultrathin graphene oxide nanofiltration membranes for water purification, *J. Mater. Chem. A*, 5 (2017) 20860-20866.
- [22] R. Li, J. Liu, A. Shi, X. Luo, J. Lin, R. Zheng, H. Fan, S.V. Selasie, H. Lin, A facile method to modify polypropylene membrane by polydopamine coating via inkjet printing technique for superior performance, *J Colloid Interface Sci*, 552 (2019) 719-727.

- [23] Y.-H. Wang, Y.-H. Wu, X. Tong, T. Yu, L. Peng, Y. Bai, X.-H. Zhao, Z.-Y. Huo, N. Ikuno, H.-Y.J.W.r. Hu, Chlorine disinfection significantly aggravated the biofouling of reverse osmosis membrane used for municipal wastewater reclamation, *Water Res*, 154 (2019) 246-257.
- [24] Y. Yuan, J.E.J.D. Kilduff, Mass transport modeling of natural organic matter (NOM) and salt during Nanofiltration of inorganic colloid-NOM mixtures, *Desalination*, 429 (2018) 60-69.
- [25] P.S. Goh, A.K. Zulhairun, A.F. Ismail, N. Hilal, Contemporary antibiofouling modifications of reverse osmosis desalination membrane: A review, *Desalination*, 468 (2019).
- [26] A. Anand, B. Unnikrishnan, J.-Y. Mao, H.-J. Lin, C.-C.J.D. Huang, Graphene-based nanofiltration membranes for improving salt rejection, water flux and antifouling—A review, *Desalination*, 429 (2018) 119-133.
- [27] G.D. Kang, Y.M. Cao, Development of antifouling reverse osmosis membranes for water treatment: A review, *Water Res*, 46 (2012) 584-600.
- [28] W. Choi, J. Choi, J. Bang, J.H. Lee, Layer-by-layer assembly of graphene oxide nanosheets on polyamide membranes for durable reverse-osmosis applications, *ACS Appl Mater Interfaces*, 5 (2013) 12510-12519.
- [29] F. Shao, L. Dong, H. Dong, Q. Zhang, M. Zhao, L. Yu, B. Pang, Y. Chen, Graphene oxide modified polyamide reverse osmosis membranes with enhanced chlorine resistance, *Journal of Membrane Science*, 525 (2017) 9-17.
- [30] X. Wang, H. Wang, Y. Wang, J. Gao, J. Liu, Y.J.D. Zhang, Hydrotalcite/graphene oxide hybrid nanosheets functionalized nanofiltration membrane for desalination, *Desalination*, 451 (2019) 209-218.
- [31] L. Liu, H. Kang, W. Wang, Z. Xu, W. Mai, J. Li, H. Lv, L. Zhao, X.J.J.o.M.S. Qian, Layer-by-layer self-assembly of polycation/GO/OCNTs nanofiltration membrane with enhanced stability and flux, *Journal of Materials Science*, 53 (2018) 10879-10890.
- [32] M. Wu, J. Yuan, H. Wu, Y. Su, H. Yang, X. You, R. Zhang, X. He, N.A. Khan, R. Kasher, Z. Jiang, Ultrathin nanofiltration membrane with polydopamine-covalent organic framework interlayer for enhanced permeability and structural stability, *Journal of Membrane Science*, 576 (2019) 131-141.
- [33] H.H. Rana, N.K. Saha, S.K. Jewrajka, A.V.R. Reddy, Low fouling and improved chlorine resistant thin film composite reverse osmosis membranes by cerium(IV)/polyvinyl alcohol mediated surface modification, *Desalination*, 357 (2015) 93-103.

- [34] H.M. Hegab, A. ElMekawy, T.G. Barclay, A. Michelmore, L. Zou, C.P. Saint, M. Ginic-Markovic, Effective in-situ chemical surface modification of forward osmosis membranes with polydopamine-induced graphene oxide for biofouling mitigation, *Desalination*, 385 (2016) 126-137.
- [35] Y. Zhan, X. Wan, S. He, Q. Yang, Y. He, Design of durable and efficient poly(arylene ether nitrile)/bioinspired polydopamine coated graphene oxide nanofibrous composite membrane for anionic dyes separation, *Chemical Engineering Journal*, 333 (2018) 132-145.
- [36] Y. He, J. Wang, H. Zhang, T. Zhang, B. Zhang, S. Cao, J. Liu, Polydopamine-modified graphene oxide nanocomposite membrane for proton exchange membrane fuel cell under anhydrous conditions, *Journal of Materials Chemistry A*, 2 (2014).
- [37] L. Huang, S. Zhao, Z. Wang, J. Wu, J. Wang, S. Wang, In situ immobilization of silver nanoparticles for improving permeability, antifouling and anti-bacterial properties of ultrafiltration membrane, *Journal of Membrane Science*, 499 (2016) 269-281.
- [38] E. Igbiginun, Y. Fennell, R. Malaisamy, K.L. Jones, V. Morris, Graphene oxide functionalized polyethersulfone membrane to reduce organic fouling, *Journal of Membrane Science*, 514 (2016) 518-526.
- [39] Y. Baek, B.D. Freeman, A.L. Zydney, J. Yoon, A Facile Surface Modification for Antifouling Reverse Osmosis Membranes Using Polydopamine under UV Irradiation, *Industrial & Engineering Chemistry Research*, 56 (2017) 5756-5760.
- [40] F. Perreault, M.E. Tousley, M. Elimelech, Thin-Film Composite Polyamide Membranes Functionalized with Biocidal Graphene Oxide Nanosheets, *Environmental Science & Technology Letters*, 1 (2013) 71-76.
- [41] A.W. Mohammad, Y.H. Teow, W.L. Ang, Y.T. Chung, D.L. Oatley-Radcliffe, N. Hilal, Nanofiltration membranes review: Recent advances and future prospects, *Desalination*, 356 (2015) 226-254.
- [42] Y. Wen, J. Yuan, X. Ma, S. Wang, Y. Liu, Polymeric nanocomposite membranes for water treatment: a review, *Environmental Chemistry Letters*, 17 (2019) 1539-1551.
- [43] V. Kochkodan, D.J. Johnson, N. Hilal, Polymeric membranes: surface modification for minimizing (bio)colloidal fouling, *Adv Colloid Interface Sci*, 206 (2014) 116-140.
- [44] V. Kochkodan, N. Hilal, A comprehensive review on surface modified polymer membranes for biofouling mitigation, *Desalination*, 356 (2015) 187-207.

- [45] S. Zinadini, A.A. Zinatizadeh, M. Rahimi, V. Vatanpour, H. Zangeneh, Preparation of a novel antifouling mixed matrix PES membrane by embedding graphene oxide nanoplates, *Journal of Membrane Science*, 453 (2014) 292-301.
- [46] J. Du, Y. Tian, N. Li, J. Zhang, W.J.P.f.A.T. Zuo, Enhanced antifouling performance of ZnS/GO/PVDF hybrid membrane by improving hydrophilicity and photocatalysis, *Polymers Advanced Technologies*, 30 (2019) 351-359.
- [47] M. Safarpour, V. Vatanpour, A.J.D. Khataee, Preparation and characterization of graphene oxide/TiO<sub>2</sub> blended PES nanofiltration membrane with improved antifouling and separation performance, *Desalination*, 393 (2016) 65-78.
- [48] X. Hao, S. Gao, J. Tian, Y. Sun, F. Cui, C.Y.J.E.s. Tang, technology, Calcium-Carboxyl Intrabridging during Interfacial Polymerization: A Novel Strategy to Improve Antifouling Performance of Thin Film Composite Membranes, *Environ Sci Technol*, 53 (2019) 4371-4379.
- [49] S.-M. Xue, C.-H. Ji, Z.-L. Xu, Y.-J. Tang, R.-H. Li, Chlorine resistant TFN nanofiltration membrane incorporated with octadecylamine-grafted GO and fluorine-containing monomer, *Journal of Membrane Science*, 545 (2018) 185-195.
- [50] G.-D. Kang, C.-J. Gao, W.-D. Chen, X.-M. Jie, Y.-M. Cao, Q.J.J.o.m.s. Yuan, Study on hypochlorite degradation of aromatic polyamide reverse osmosis membrane, *Journal of Membrane Science*, 300 (2007) 165-171.
- [51] J.-H. Lee, J.Y. Chung, E.P. Chan, C.M.J.J.o.m.s. Stafford, Correlating chlorine-induced changes in mechanical properties to performance in polyamide-based thin film composite membranes, *Journal of Membrane Science*, 433 (2013) 72-79.
- [52] J.-E. Gu, B.-M. Jun, Y.-N.J.W.r. Kwon, Effect of chlorination condition and permeability of chlorine species on the chlorination of a polyamide membrane, *Water Res*, 46 (2012) 5389-5400.
- [53] H.M. Colquhoun, D. Chappell, A.L. Lewis, D.F. Lewis, G.T. Finlan, P.J.J.J.o.M.C. Williams, Chlorine tolerant, multilayer reverse-osmosis membranes with high permeate flux and high salt rejection, *Journal of Materials Chemistry*, 20 (2010) 4629-4634.